Dynamical Glass and Ergodization Times in Classical Josephson Junction Chains

Thudiyangal Mithun,[1] Carlo Danieli,[1] Yagmur Kati,[1,2] and Sergej Flach[1]

[1]*Center for Theoretical Physics of Complex Systems, Institute for Basic Science, Daejeon 34051, Korea*
[2]*Basic Science Program, Korea University of Science and Technology (UST), Daejeon 34113, Republic of Korea*

Models of classical Josephson junction chains turn integrable in the limit of large energy densities or small Josephson energies. Close to these limits the Josephson coupling between the superconducting grains induces a short-range nonintegrable network. We compute distributions of finite-time averages of grain charges and extract the ergodization time T_E which controls their convergence to ergodic δ distributions. We relate T_E to the statistics of fluctuation times of the charges, which are dominated by fat tails. T_E is growing anomalously fast upon approaching the integrable limit, as compared to the Lyapunov time T_Λ—the inverse of the largest Lyapunov exponent—reaching astonishing ratios $T_E/T_\Lambda \geq 10^8$. The microscopic reason for the observed dynamical glass is rooted in a growing number of grains evolving over long times in a regular almost integrable fashion due to the low probability of resonant interactions with the nearest neighbors. We conjecture that the observed dynamical glass is a generic property of Josephson junction networks irrespective of their space dimensionality.

Ergodicity is a core concept of statistical physics of many-body systems. It demands infinite-time averages of observables during a microcanonical evolution to match with their proper phase space averages [1]. Any laboratory or computational experiment is, however, constrained to finite averaging times. Are these sufficient or not? How much time is needed for a trajectory to visit the majority of the available microcanonical states, and for the finite-time average of an observable to be reasonably close to its statistical average? Can we define an *ergodization* timescale T_E on which these properties manifest? What is that ergodization time depending on? Doubts on the applicability of the ergodic hypothesis itself were discussed for such simple cases as a mole of Ne at room temperature (see Ref. [2], and references therein). Glassy dynamics have been reported in a large variety of Hamiltonian systems [3–6]. Further, spin glasses [7] and stochastic Levy processes [8–13] reveal that the ergodization time (and even ergodicity itself) may be affected by heavy-tailed distributions of lifetimes of typical excitations. The aim of this work is to address the above issues using a simple and paradigmatic dynamical many-body system test bed.

Josephson junction networks are devices that are known for their wide applicability over various fields, such as superconductivity, cold atoms, optics, and metamaterials, among others [14–16] (for a recent survey on experimental results, see Ref. [17]): synchronization has been studied in Refs. [18,19], discrete breathers were observed and studied in Refs. [20–23], qubit dynamics was analyzed in Refs. [24,25], and the thermal conductivity was computed in Refs. [26,27]. In particular, a recent study conducted by Pino *et al.* [28] showed the existence of a nonergodic or bad metal region in the high-temperature regime of a quantum chain of Josephson junctions, that exists as a prelude to a many-body localization phase [29]. Notably, in Ref. [28] it has been conjectured that the bad metal regime persists as a nonergodic phase in the classical limit of the model—the large energy density regime of a chain of coupled rotors, close to an integrable limit. A similar prediction of a nonergodic phase (called the weak coupling phase) in the same model was obtained in Ref. [30]. Further, in Ref. [31], a faster decay of thermal conductivity in the high-temperature regime is observed. On the other side, a strong slowing-down of relaxations has been identified in the proximity of such a limit if the nonintegrable perturbation spans a short-range network between corresponding actions [32]. The limit of weak Josephson coupling or high temperature corresponds precisely to that short-range network case. Is the Josephson junction chain then ergodic or not?

In this Letter we demonstrate the existence of a dynamical glass in a classical Josephson junction chain of coupled rotors. We evaluate the convergence of distributions of finite-time averages of the superconducting grain charges and extract an ergodization timescale T_E. We show that this timescale is related to the properties of the statistics of charge fluctuation times. Such fluctuation event statistics was introduced in Refs. [32,33]. We compute the Lyapunov time T_Λ—the inverse of the largest Lyapunov exponent Λ [34,35]. The Lyapunov time is a lower bound for the ergodization time: $T_\Lambda \leq T_E$. In the reported dynamical glass, the dynamics stays ergodic and T_E is finite. However, T_E is growing anomalously fast upon approaching the integrable limit, as compared to T_Λ reaching astonishing

ratios $T_E/T_\Lambda \geq 10^8$. We show that T_E is controlled by fat tails of charge fluctuation time distributions. We compute the spatiotemporal evolution of nonlinear resonances between interacting grains [30,36]. The microscopic reason for the observed dynamical glass is rooted in a growing number of grains evolving over long times in a regular almost integrable fashion due to the low probability of resonant interactions with nearest neighbors. The dynamical glass behavior is expected to be a generic property of a large class of dynamical systems, where ergodization timescales depend sensitively on control parameters. At the same time, the concept of ergodicity is preserved, and statistical physics continues to work—it is all just a matter of timescales.

We consider the Hamiltonian

$$H(q,p) = \sum_{n=1}^{N} \left(\frac{p_n^2}{2} + E_J[1 - \cos(q_{n+1} - q_n)] \right), \quad (1)$$

describing the dynamics of a chain of N superconducting islands with weak nearest neighbor Josephson coupling in its classical limit. We note that this model is equivalent to an XY chain or similarly to a coupled rotor chain, where the grain charging energies turn into the above kinetic energy terms [28,36]. We apply periodic boundary conditions $p_1 = p_{N+1}$ and $q_1 = q_{N+1}$ for the conjugate angles q_n and momenta p_n. E_J controls the strength of Josephson coupling. The corresponding equations of motion of Eq. (1) are

$$\dot{q}_n = p_n, \quad \dot{p}_n = E_J[\sin(q_{n+1} - q_n) + \sin(q_{n-1} - q_n)]. \quad (2)$$

This system has two conserved quantities: the total energy H and the total angular momentum $L = \sum_{n=1}^{N} p_n$. We will choose $L = 0$ without loss of generality. Exact expressions for average full h and kinetic k energy densities as functions of temperature are obtained using a Gibbs distribution [37] and yield

$$h = k + E_J \left(1 - \frac{I_1(E_J/2k)}{I_0(E_J/2k)} \right), \quad (3)$$

with $I_{0,1}$ being the modified Bessel functions of the first kind. We investigate the equilibrium dynamics of the above system in proximity to two integrable limits: $h \to \infty$ or $E_J \to 0$. At these limits, the system reduces to a set of uncoupled superconducting grains $H_0 = \sum_{n=1}^{N}(p_n^2/2)$ [36]. In proximity to these limits, the Josephson terms induce a nonintegrable perturbation through a short-range interaction network of actions $\{p_n\}_n$ [32]. We consider the kinetic energies $k_n = p_n^2/2$ as a set of time-dependent observables. Because of the discrete translational invariance of H, all k_n variables are statistically equivalent, fluctuating around their equilibrium value k. We will integrate the equations of motion using symplectic
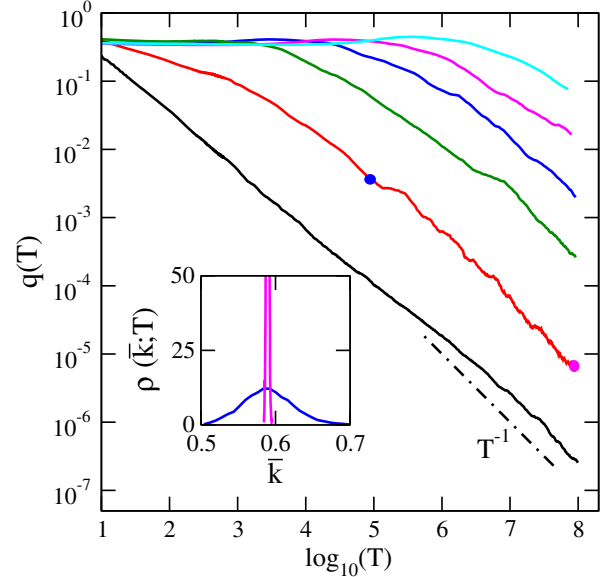

FIG. 1. (a) Fluctuation index $q(T)$ for energy densities (bottom to top) 0.1 (black), 1.2 (red), 2.4 (green), 3.8 (blue), 5.4 (magenta), and 8.5 (cyan). Inset: $\rho(\bar{k}; T)$ for $h = 1.2$ and two different times $T = 10^5$ (blue circle) and $T = 10^8$ (magenta circle) marked in the main plot. Here, $E_J = 1$ and the number of realizations $R = 12$ for all data.

integrators [37]. Unless otherwise stated, we use the system size $N = 2^{10}$.

To quantitatively assess the ergodization time T_E, we compute finite-time averages $\bar{k}_{n,T} = (1/T) \int_0^T k_n(t)dt$ for a set of R different trajectories at given h, E_J. The corresponding distribution $\rho(\bar{k}; T)$ is characterized by its first moment $\mu_k(T)$ and the standard deviation $\sigma_k(T)$. Assuming ergodicity, $\mu_k(T \to \infty) = k$ and $\sigma_k(T \to \infty) = 0$, since the distribution $\rho(\bar{k}; T \to \infty) = \delta(\bar{k} - k)$. In the inset of Fig. 1, we show the distributions $\rho(\bar{k}; T)$ for $h = 1.2$ at two different averaging times $T = 10^5$, 10^8. As expected, the distribution $\rho(\bar{k}, T)$ converges to a delta function, centered around k. We then use the fluctuation index $q(T) = [\sigma_k^2(T)/\mu_k^2(T)]$ as a quantitative dimensionless measure of the above convergence properties.

In Fig. 1, we show $q(T)$ for different values of h with $E_J = 1$. We find $q(T \ll T_E) = q(0)$ and $q(T \gg T_E) \sim T_E/T$, where T_E is our definition of the ergodization timescale. We rescale and fit the different curves $q(T)$ and extract T_E [37]. The result is plotted in Fig. 3(a) with green squares. T_E quickly grows by orders of magnitude upon increasing the energy density h in a rather moderate window of values, close to a power law $T_E \sim h^6$. When fixing $h = 1$ and varying E_J, we make similar observations [37], with $T_E \sim E_J^{-6.5}$, as shown in Fig. 3(b). With our results, we validate ergodic dynamics in the considered system. Previous reports [28,30] did not address the quickly growing timescale T_E upon approaching the integrable limit.
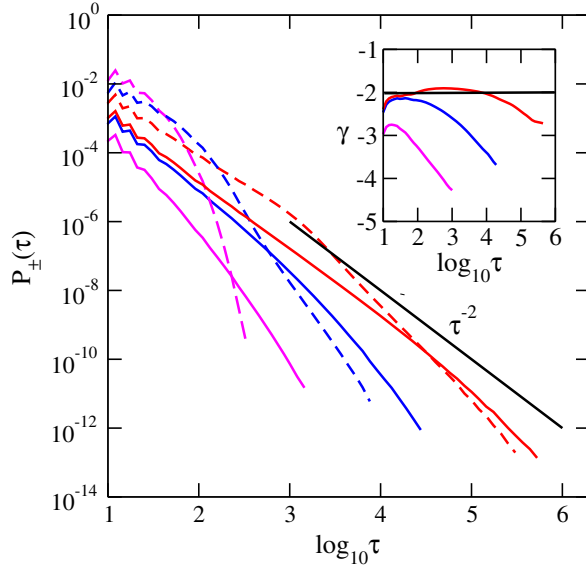
FIG. 2. $P_+(\tau)$ (solid lines) and $P_-(\tau)$ (dashed lines) for various energy densities $h = 1.2$ (magenta), $h = 2.4$ (blue), and $h = 5.4$ (red). Here, $E_J = 1$. The black line corresponds to a power law decay τ^{-2} and guides the eye. Inset: $\gamma \equiv d(\log_{10} P_+)/d(\log_{10} \tau)$. The black solid horizontal line guides the eye at value -2.

Let us study the fluctuation statistics of the observables $k_n(t)$. Each of them has to fluctuate around their common average k. This allows us to segment the trajectory of the whole system phase space into consecutive excursions [32,33]. Note that for each site n the segmenting is different, and we account for all of them. We measure the consecutive piercing times t_n^i at which $k_n(t) = k$. We then compute the *excursion times* $\tau_n^\pm(i) = t_n^{i+1} - t_n^i$ for a trajectory of excursion events during which $k(t) > k$ (τ^+) and $k(t) < k$ (τ^-), respectively. Figure 2 shows the distributions for $E_J = 1$ and various energy densities h. As h increases, both distributions increase their tail weights, with P_+ dominating over P_-. Further, the distributions develop intermediate tail structures close to a $1/\tau^2$ (see inset in Fig. 2).

We can now compute the following two timescales: the average excursion time μ_τ and the standard deviation σ_τ of the distribution P_+, which are shown in Fig. 3(a) (orange diamonds and blue triangles) as functions of h. We observe that σ_τ equals with μ_τ at $h \approx 1$ and quickly overgrows μ_τ for $h > 1$, signaling the proximity to an integrable limit, where the dynamics is dominated by fluctuations rather than the means. Indeed, if the distributions $P_\pm(\tau)$ asymptotically reach a $1/\tau^2$ dependence in the integrable limit, then not only the timescales μ_τ and σ_τ have to diverge, but their ratio σ_τ/μ_τ will diverge as well.

The above timescales are related to the ergodization timescale T_E as

$$T_E \sim \tau_q \equiv \frac{\sigma_\tau^2}{\mu_\tau}. \qquad (4)$$
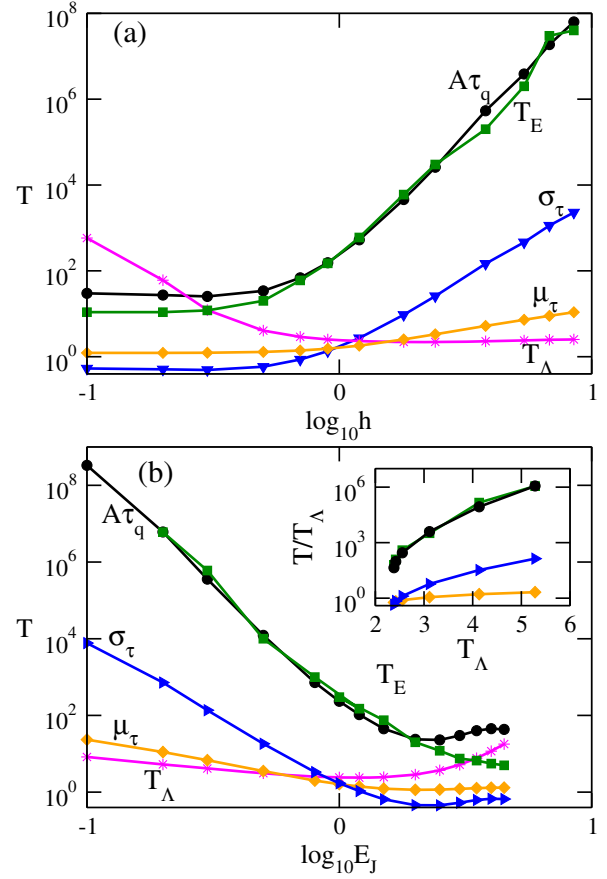

FIG. 3. (a) Timescales T_E (green squares), $A\tau_q$ (black circles), Lyapunov time T_Λ (magenta stars), μ_τ (orange diamonds), and σ_τ (blue triangles) vs the energy density h for $E_J = 1$ and $A = 130$. (b) Same as in (a) but vs E_J at the fixed energy density $h = 1$. Inset: Rescaled times ($A\tau_q$, T_E, m_τ, and σ_τ) in units of the Lyapunov time T_Λ.

This relation can be obtained, e.g., after approximating the dependence $k_n(t)$ by a telegraph random process with excursion time distributions $P_\pm$ [37]. We plot $A\tau_q$ vs h in Fig. 3(a) (black circles) with a fitting parameter $A = 130$. The curve is strikingly close to the dependence $T_E(h)$ for $h > 1$. We thus independently reconfirm that the considered system dynamics is ergodic, yet with quickly growing timescales of ergodization. When fixing $h = 1$ and varying E_J, we make similar observations as shown in Fig. 3(b). The physical origin of A is an interesting and open question for future studies.

With ergodicity being restored, the question remains: what is the microscopic origin of the enormously fast growing ergodization time? Since the considered system is nonintegrable, its dynamics must be chaotic. Therefore there is a Lyapunov timescale $T_\Lambda = 1/\Lambda$ dictated by the largest Lyapunov exponent Λ. T_Λ can be expected to serve as a lower bound for the ergodization timescale. We compute Λ using standard techniques [37] and also compare it with theoretical predictions [34,35]. We plot
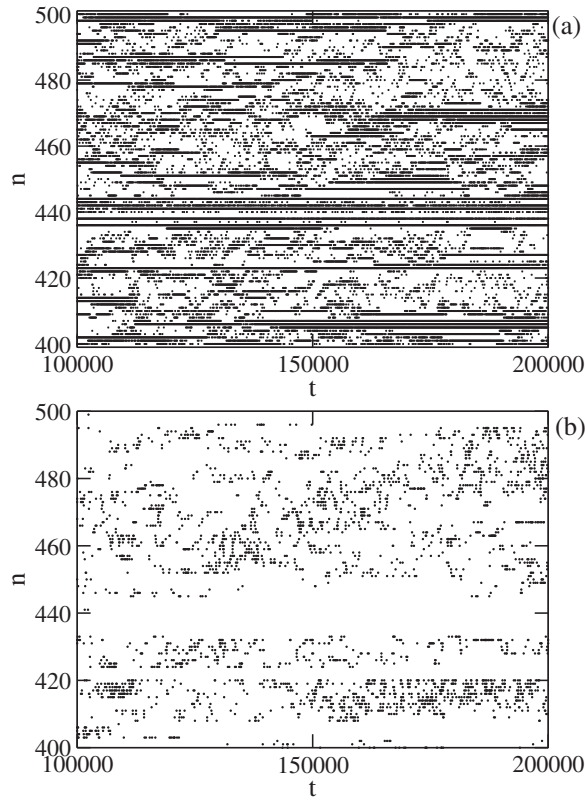
FIG. 4. (a) Spatiotemporal evolution of a part of the Josephson junction chain for $E_J = 1$ and $h = 5.4$. Black points correspond to events with $k_n > k$. (b) Spatiotemporal evolution of nonlinear resonances for the same parameters as in (a). See text for details.

the Lyapunov time T_Λ vs h in Fig. 3(a) and vs E_J in Fig. 3(b) (magenta stars). The surprising finding is that $T_\Lambda \lesssim \mu_\tau$, in proximity to the integrable limit. Thus, $T_\Lambda \ll T_E$; e.g., for $E_J = 1$ and $h = 10$ we find $T_\Lambda \sim 1$ and $T_E \sim 10^8$. The inset of Fig. 3(b) demonstrates the above findings where $T_E, A\tau_q, \mu_\tau$, and σ_τ are plotted vs T_Λ and in units of T_Λ. These are typical features of the novel dynamical glass, which starts at $h \approx E_J$.

In order to advance, we analyze the spatiotemporal dynamics of $k_n(t)$ in Fig. 4(a). We plot black points during events $k_n(t) > k$ for $E_J = 1$ and $h = 5.4$ over a time window of 10^5 and a spatial window of 100 sites. We observe many long-lasting events, which slowly diffuse in space. At the same time, regions between these long-lasting events appear to be more chaotic, with this chaos however being confined to regions between two events. The events correspond to long-living breatherlike excitations [32]. The existence of chaotic spots was predicted in Refs. [28,30]. We then compute the frequency difference $\Delta_n = |\omega_n - \omega_{n+1}|$ between neighboring grains, where $\omega_n = \dot{q}_n = p_n$. Following Refs. [28,30,42], we define a chaotic resonance if a neighboring pair $\Delta_n < 1$ and $\Delta_{n+1} < 1$. We plot the spatiotemporal evolution of these nonlinear resonances in Fig. 4(b) with the resonances

marked with black dots. We observe a slowly diffusing and meandering network of chaotic puddles.

The large ergodization time T_E could be related to a small density of chaotic spots and/or to a weak interaction between the spots. The density of chaotic spots was calculated in Ref. [30] as $D = (1/\sqrt{\pi}) \int_0^y e^{-x^2} dx$, where $y = \sqrt{16\beta/3}$ for $E_J = 1$ and β is the inverse temperature [37]. Note that $1/\beta \approx 2h$ for $h \gg 1$. It follows that $D \sim 1/\sqrt{h}$ for $h \gg 1$. This decay is way too slow to explain the rapid increase of the ergodization time T_E upon increasing h in Fig. 3(a). There, h increases by 1 order of magnitude, D decreases by a factor of 3, but T_E increases by 6 orders of magnitude. Therefore, the ergodization time in the dynamical glass must be controlled by a very weak interaction between chaotic spots, which have to penetrate silent nonchaotic regions formed by breatherlike events.

To conclude, the classical dynamics of a Josephson junction chain at large temperatures (i.e., energy densities) or likewise at weak Josephson coupling is characterized by a dynamical glass in its proximity to corresponding integrable limits. This dynamical glass is induced by the short range of the nonintegrable perturbation network spanned between the actions which turn integrals of motion at the very integrable limit. The dynamics of the system remains ergodic, albeit with rapidly increasing ergodization time T_E. We relate T_E to timescales extracted from the fluctuations of the actions. We also show that the Lyapunov time, which is marking the onset of chaos in the system, is orders of magnitude shorter than T_E. The reason for the rapidly growing ergodization time is rooted in the slowing-down of interactions between chaotic spots. By virtue of the short-range network we expect our results to hold as well in higher space dimensions. A highly nontrivial and interesting question is the relation of the dynamical glass to the Kolmogorov-Arnold-Moser (KAM) regime [43–45]. Common expectations tell us that the KAM regime thresholds of a nonintegrable perturbation vanish very fast with an increasing number of degrees of freedom N, perhaps even exponentially fast due to proliferating resonances [46–49]. The long-lasting regular motion in the dynamical glass is local both in space and time, as manifested by the exponential cutoff tails in Fig. 2. The dynamical glass appears is originated from a chaotic component of measure one in the available phase space. This is very different from few degree of freedom systems with a mixed phase space. A quantitative theory for the dependence of the ergodization time on the control parameters in the proximity of the discussed integrable limits is a challenging future task, and as intriguing as the question about the fate of the dynamical glass in the related quantum many-body problem.

[1] A. J. Lichtenberg and M. A. Lieberman, *Regular and Chaotic Dynamics*, Applied Mathematical Sciences (Springer, Berlin, 1992), Vol. 38.

[2] B. Gaveau and L. S. Schulman, Is ergodicity a reasonable hypothesis for macroscopic systems?, Eur. Phys. J. **224,** 891 (2015).

[3] G. Biroli and M. Tarzia, Delocalized glassy dynamics and many-body localization, Phys. Rev. B **96,** 201114 (2017).

[4] C. Pérez-Espigares, F. Carollo, J. P. Garrahan, and P. I. Hurtado, Dynamical criticality in driven systems: Non-perturbative results, microscopic origin and direct observation, Phys. Rev. E **98,** 060102 (2018).

[5] H. Tong and H. Tanaka, Revealing Hidden Structural Order Controlling Both Fast and Slow Glassy Dynamics in Supercooled Liquids, Phys. Rev. X **8,** 011041 (2018).

[6] A. Senanian and O. Narayan, Glassy dynamics in disordered oscillator chains, Phys. Rev. E **97,** 062110 (2018).

[7] J.-P. Bouchaud, Weak ergodicity breaking and aging in disordered systems, J. Phys. I **2,** 1705 (1992).

[8] G. Bel and E. Barkai, Weak Ergodicity Breaking in the Continuous-Time Random Walk, Phys. Rev. Lett. **94,** 240602 (2005).

[9] G. Bel and E. Barkai, Weak ergodicity breaking with deterministic dynamics, Europhys. Lett. **74,** 15 (2006).

[10] A. Rebenshtok and E. Barkai, Distribution of Time-Averaged Observables for Weak Ergodicity Breaking, Phys. Rev. Lett. **99,** 210601 (2007).

[11] A. Rebenshtok and E. Barkai, Weakly non-ergodic statistical physics, J. Stat. Phys. **133,** 565 (2008).

[12] N. Korabel and E. Barkai, Pesin-Type Identity for Intermittent Dynamics with a Zero Lyapunov Exponent, Phys. Rev. Lett. **102,** 050601 (2009).

[13] J. H. P. Schulz and E. Barkai, Fluctuations around equilibrium laws in ergodic continuous-time random walks, Phys. Rev. E **91,** 062129 (2015).

[14] F. S. Cataliotti, S. Burger, C. Fort, P. Maddaloni, F. Minardi, A. Trombettoni, A. Smerzi, and M. Inguscio, Josephson junction arrays with Bose-Einstein condensates, Science **293,** 843 (2001).

[15] C. Ryu, P. W. Blackburn, A. A. Blinova, and M. G. Boshier, Experimental Realization of Josephson Junctions for an Atom SQUID, Phys. Rev. Lett. **111,** 205301 (2013).

[16] M. C. Cassidy, A. Bruno, S. Rubbert, M. Irfan, J. Kammhuber, R. N. Schouten, A. R. Akhmerov, and L. P. Kouwenhoven, Demonstration of an ac Josephson junction laser, Science **355,** 939 (2017).

[17] J. A. Blackburn, M. Cirillo, and N. Grønbech-Jensen, A survey of classical and quantum interpretations of experiments on Josephson junctions at very low temperatures, Phys. Rep. **611,** 1 (2016).

[18] D. Tsygankov and K. Wiesenfeld, Spontaneous synchronization in a Josephson transmission line, Phys. Rev. E **66,** 036215 (2002).

[19] H. F. El-Nashar, Y. Zhang, H. A. Cerdeira, and A. F. Ibiyinka, Synchronization in a chain of nearest neighbors coupled oscillators with fixed ends, Chaos **13,** 1216 (2003).

[20] P. Binder, D. Abraimov, A. V. Ustinov, S. Flach, and Y. Zolotaryuk, Observation of Breathers in Josephson Ladders, Phys. Rev. Lett. **84,** 745 (2000).

[21] A. E. Miroshnichenko, S. Flach, M. V. Fistul, Y. Zolotaryuk, and J. B. Page, Breathers in Josephson junction ladders: Resonances and electromagnetic wave spectroscopy, Phys. Rev. E **64,** 066601 (2001).

[22] M. V. Fistul, A. E. Miroshnichenko, S. Flach, M. Schuster, and A. V. Ustinov, Incommensurate dynamics of resonant breathers in Josephson junction ladders, Phys. Rev. B **65,** 174524 (2002).

[23] A. E. Miroshnichenko, M. Schuster, S. Flach, M. V. Fistul, and A. V. Ustinov, Resonant plasmon scattering by discrete breathers in Josephson junction ladders, Phys. Rev. B **71,** 174306 (2005).

[24] K. V. Shulga, E. Il'ichev, M. V. Fistul, I. S. Besedin, S. Butz, O. V. Astafiev, U. Hübner, and A. V. Ustinov, Magnetically induced transparency of a quantum metamaterial composed of twin flux qubits, Nat. Commun. **9,** 150 (2018).

[25] J. M. Martinis, Superconducting qubits and the physics of Josephson junctions, in *Quantum Entanglement and Information Processing*, edited by D. Estéve, J.-M. Raimond, and J. Dalibard (Elsevier, New York, 2004), Vol. 79, pp. 487–520.

[26] O. V. Gendelman and A. V. Savin, Normal Heat Conductivity of the One-Dimensional Lattice with Periodic Potential of Nearest-Neighbor Interaction, Phys. Rev. Lett. **84,** 2381 (2000).

[27] C. Giardinà, R. Livi, A. Politi, and M. Vassalli, Finite Thermal Conductivity in 1D Lattices, Phys. Rev. Lett. **84,** 2144 (2000).

[28] M. Pino, L. B. Ioffe, and B. L. Altshuler, Nonergodic metallic and insulating phases of Josephson junction chains, Proc. Natl. Acad. Sci. U.S.A. **113,** 536 (2016).

[29] D. Basko, I. Aleiner, and B. Altshuler, Metal insulator transition in a weakly interacting many-electron system with localized single-particle states, Ann. Phys. (Amsterdam) **321,** 1126 (2006).

[30] D. Escande, H. Kantz, R. Livi, and S. Ruffo, Self-consistent check of the validity of Gibbs calculus using dynamical variables, J. Stat. Phys. **76,** 605 (1994).

[31] W. De Roeck and F. Huveneers, Asymptotic localization of energy in nondisordered oscillator chains, Commun. Pure Appl. Math. **68,** 1532 (2015).

[32] T. Mithun, Y. Kati, C. Danieli, and S. Flach, Weakly Nonergodic Dynamics in the Gross-Pitaevskii Lattice, Phys. Rev. Lett. **120,** 184101 (2018).

[33] C. Danieli, D. K. Campbell, and S. Flach, Intermittent many-body dynamics at equilibrium, Phys. Rev. E **95,** 060202 (2017).

[34] L. Casetti, C. Clementi, and M. Pettini, Riemannian theory of Hamiltonian chaos and Lyapunov exponents, Phys. Rev. E **54,** 5969 (1996).

[35] L. Casetti, M. Pettini, and E. Cohen, Geometric approach to Hamiltonian dynamics and statistical mechanics, Phys. Rep. **337,** 237 (2000).

[36] R. Livi, M. Pettini, S. Ruffo, and A. Vulpiani, Chaotic behavior in nonlinear Hamiltonian systems and equilibrium statistical mechanics, J. Stat. Phys. **48,** 539 (1987).

[37] See Supplemental Material at http://link.aps.org/supplemental/10.1103/PhysRevLett.122.054102 for for numerical details and ergodization time calculations and it includes Refs. [38–41].

[38] C. Skokos, D. O. Krimer, S. Komineas, and S. Flach, Delocalization of wave packets in disordered nonlinear chains, Phys. Rev. E **79**, 056211 (2009).

[39] R. P. Feynman, Statistical mechanics, a set of lectures, Am. J. Phys. **42**, 620 (1974).

[40] S. Chakravarty and S. Kivelson, Photoinduced macroscopic quantum tunneling, Phys. Rev. B **32**, 76 (1985).

[41] M. Kac, G. Uhlenbeck, and P. Hemmer, On the van der Waals theory of the vapor-liquid equilibrium. I. Discussion of a one-dimensional model, J. Math. Phys. (N.Y.) **4**, 216 (1963).

[42] B. V. Chirikov, A universal instability of many-dimensional oscillator systems, Phys. Rep. **52**, 263 (1979).

[43] A. N. Kolmogorov, On conservation of conditionally periodic motions for a small change in Hamilton's function, Dokl. Akad. Nauk SSSR **98**, 527 (1954) [LNP **93**, 51 (1979)].

[44] V. Arnold, A proof of a theorem by a.n. kolmogorov on the invariance of quasi-periodic motions under small perturbations of the Hamiltonian, Russ. Math. Surv. **18**, 9 (1963).

[45] J. Moser, On invariant curves of area-preserving mappings of an annulus, Nachr. Akad. Wiss. Goettingen 2, **6**, 1 (1962).

[46] L. Chierchia and G. Gallavotti, Smooth prime integrals for quasi-integrable Hamiltonian systems, Il Nuovo Cimento B **67**, 277 (1982).

[47] G. Benettin, L. Galgani, A. Giorgilli, and J. M. Strelcyn, A proof of Kolmogorov's theorem on invariant tori using canonical transformations defined by the Lie method, Il Nuovo Cimento B **79**, 201 (1984).

[48] C. E. Wayne, The KAM theory of systems with short range interactions, 1, Commun. Math. Phys. **96**, 311 (1984).

[49] C. E. Wayne, The KAM theory of systems with short range interactions, 2, Commun. Math. Phys. **96**, 331 (1984).